Kinetic energy effects on morphology evolution during pulsed laser deposition of metal-on-insulator films

Jeffrey M. Warrender* and Michael J. Aziz
Division of Engineering and Applied Sciences, Harvard University, Cambridge, Massachusetts 02138, USA
(Received 2 November 2006; revised manuscript received 29 December 2006)

We report an experimental comparison of Volmer-Weber metal-on-insulator growth morphology in pulsed laser deposition (PLD) and thermal deposition under identical thermal, background, and surface preparation conditions for Ag on SiO_2 and mica. Films exhibit a characteristic morphological progression from isolated three-dimensional islands to elongated clusters to a percolating, electrically conducting film to a pinhole-free film. We observed this same progression for films deposited by PLD. Kinetic Monte Carlo (KMC) simulations that take into account only the pulsed nature of the flux predict that PLD films should advance to percolation with less deposition than thermally deposited films under otherwise identical conditions. At low substrate temperatures, this prediction is confirmed. However, *in situ* resistance measurements and *ex situ* atomic force microscopy measurements demonstrate that at high substrate temperatures, PLD films require *more* deposition to reach percolation. PLD experiments performed at varying kinetic energy of the depositing Ag species suggest a regime in which increasing kinetic energy can delay the percolation transition. Comparison was made with KMC simulations of two-island coalescence in the presence of adatom-vacancy pair creation, which occurs with a greater-than-unity yield per incident ion at kinetic energy >50 eV. A mechanism controlling the delayed percolation of PLD films in the high-temperature regime is proposed: (1) the energetic deposition results in a net uphill flux from adatom-vacancy pair creation, inducing a vertical shape change; (2) taller-than-equilibrium islands coalesce more rapidly; (3) the result is an extended time period over which coalescence is efficient compared to island-island impingement; (4) the percolation transition is delayed.

DOI: XXXX PACS number(s): 81.15.Fg, 68.55.−a, 81.07.Bc, 82.20.Wt

I. INTRODUCTION

The formation of nonwetting three-dimensional (3D) islands on an otherwise bare surface in the early stages of thin-film deposition, termed the Volmer-Weber growth mode, is a very common observation in the integration of dissimilar materials. An exemplary case is the deposition of metals on insulators.[1–5] The delay, by kinetic processes occurring on the surface, of the morphology evolution with increasing deposition toward a uniform, pinhole-free film has often been treated as a nuisance. Recent discoveries of surface plasmon-enhanced phenomena present opportunities for the exploitation of nanoparticulate and nanoporous metal films, e.g., in enhancing semiconductor quantum dot luminescence.[6,7]

In the absence of singular surface energetics, for nonwetting islands thermodynamics favors sufficiently large islands over a flat, contiguous film. The morphology evolution sequence exhibits complex kinetics. The initial stage of deposition is characterized by the nucleation and growth of isolated 3D islands. As the islands grow larger, they impinge upon each other. Upon impingement, islands begin to *coalesce*, driven by capillary forces toward a more equiaxed equilibrium shape,[8] delaying the development of a contiguous film. The time required for this process increases with increasing island size.[9] For a given system of two or more coalescing islands, which we refer to as a *coalescing cluster* (or just "cluster"), there is an island size above which the time required for coalescence exceeds the average time interval before an additional island impinges with one of the constituent islands in the cluster. It is beyond this point that clusters of coalescing islands remain elongated on the surface; they have become *kinetically frozen*.[3] Further deposition joins these elongated clusters, forming a tortuous network of island chains that conducts electrically (the "percolation transition"); with further deposition, the intervening bare channels continue to fill in until no pinholes remain.[2]

The extensive knowledge base on metal-on-insulator film grow by thermal deposition makes an excellent model system with which to study surface kinetics in film growth by pulsed laser deposition (PLD). PLD differs from thermal deposition in at least two essential ways: (1) although the average deposition rates are similar, in PLD the depositing species arrive in short bursts, on the order of 10–100 μs, and (2) the depositing species have kinetic energies of 10–100 eV, compared with about 1 eV for thermally grown films.[10,11]

We have previously reported the results of nonenergetic kinetic Monte Carlo (KMC) simulations in an investigation of the effect of flux pulsing on the rate of advancement through the characteristic morphology progression. Based on this work, pulsed deposition is expected to lead to elongation and, subsequently, percolation, with less deposition than that in continuous deposition at the same temperature and average flux.[12] This occurs because at the early stages, the islands grown by pulsed deposition are smaller and more densely spaced than those for the continuous case, as a result of the higher instantaneous deposition rate in PLD. Assuming that the islands maintain their shape and contact angle during growth, 3D islands that are smaller and closer together will require relatively less material to grow to the point of impingement. A brief note about our terminology: for compactness, we use the term "percolates sooner (later)" to mean

"requires less (more) deposition to reach the percolation transition at the same temperature and average deposition flux."

In the present work, *ex situ* atomic force microscopy (AFM) and *in situ* lateral electrical resistance measurements were performed to compare the percolation thickness in PLD and in thermal deposition at the same average deposition rate under identical background gas, thermal, and substrate preparation conditions. We find that under some conditions, PLD films percolate sooner than do thermally deposited films, consistent with the aforementioned KMC simulations that accounted only for effect (1), the time structure of the deposition flux. However, we find other conditions in which PLD films percolate later than thermally deposited films. Mechanisms resulting from energetic effect (2) are investigated, and, when incorporated into a detailed KMC model, are found to induce a shape change in the islands, making them taller than in equilibrium. These taller-than-equilibrium islands are found to coalesce more rapidly than islands with the equilibrium aspect ratio. We propose this scenario as an explanation of the delay in the percolation transition observed for PLD compared to thermal deposition.

II. EXPERIMENT

Ag films were prepared by PLD in a vacuum chamber with base pressure of 2×10^{-8} Torr. The target was 99.999% pure Ag and was irradiated with a KrF^+ excimer laser beam (Lambda Physik LPX 305), with wavelength of 248 nm and pulse duration of 30 ns full width at half-maximum, at a pulse frequency of 10–33 Hz as required to achieve the desired fluence and average deposition rate. The target was rotated during deposition and was irradiated for 2 min at 10 Hz for target cleaning prior to each growth run. The substrate was SiO_2 or muscovite mica (freshly cleaved in deionized water), mounted 10.5 or 6.5 cm from the target, respectively. Thermally grown films were deposited in the same chamber with a homebuilt deposition source consisting of a 0.25 mm Ag foil, 99.999% pure, irradiated with a tungsten filament located 2 mm behind the foil. The current in the filament was 9 A, resulting in a foil temperature of about 900 °C. The deposition rate was 0.06 nm/s. The substrates were attached with molten In to a metal substrate holder which was heated from the back side resistively and controlled at temperatures from 40 to 225 °C. Immediately upon the cessation of deposition, the heater power was disconnected and films were allowed to cool to room temperature, at a rate of approximately ~0.5 °C/s. Growth morphologies were characterized by *ex situ* AFM.

The onset of the electrical percolation transition was monitored on the SiO_2 films with an *in situ* resistance measurement. In order to make good electrical contact with the growing film, Ag contact pads, 300 nm thick, were deposited onto the substrate surface in a thermal evaporator. A shadow mask was used to produce two square pads, 0.64 cm on a side and 0.64 mm apart. Indium drops were applied to each of these pads, and Au-tipped contact probes were embedded in the In while it was molten. Each probe was plugged into a gold-coated receptacle and was connected by a wire to an electrical feedthrough. The resistance measurement was performed by a Keithley 2000 digital multimeter, in the "4 Wire Resistance" mode. The resistance was recorded once per second. Based on the work of So *et al.*, it is expected that when the metal film reaches percolation, a precipitous drop in the resistance will be observed.[13] In Fig. 1(a), we show the resistance as a function of film thickness for a representative PLD and thermal deposition. In both cases, the drop in resistance that indicates electrical continuity is evidenced as a dramatic change in the slope of the resistance curve that results in a drop in resistance of at least an order of magnitude. We identified the thickness at the midpoint of this steeply sloped region.

III. EXPERIMENTAL RESULTS

A. PLD vs thermal deposition

The percolation thickness, determined by in situ electrical resistance measurements, vs substrate temperature is compared for PLD and thermally deposited films on SiO_2 in Figs. 1(b) and 1(c). Two different values of the laser fluence are compared to the same data for thermally deposited films in the two separate panels. The laser fluence was 4.6 J/cm^2 for the PLD runs shown in (b) and 6 J/cm^2 for the PLD runs shown in (c), which gave kinetic energies of 55 and 110 eV, respectively, as measured by a time-of-flight (TOF) ion probe. Figure 2 shows a representative ion probe trace. Note that throughout the remainder of the paper, our use of the term "kinetic energy" refers to the energy calculated for the peak of the TOF distribution measured with the ion probe. We estimate a possible measurement error in true thickness of about 6%. Additionally, a possible run-to-run variation in deposition rate of at most 10% contributes an uncertainty in percolation thickness of about 3% because the percolation thickness is proportional to the $-1/3$ power of the flux.[12] Combining these two effects leads to a possible error in the calculated percolation thickness of about 7%. The measured temperature scale has a possible systematic error of ±20 °C. All films were deposited at an average deposition rate F of 0.06±0.005 nm/s, with the exception of the PLD points in Fig. 1(c) at 77, 112, 122, and 200 °C, which were deposited at 0.04±0.005 nm/s. The error bars on these points indicate the direction and magnitude of the correction that would result from rescaling these measured percolation thicknesses by $F^{-1/3}$. Finally, to maintain a constant average deposition rate, the pulse rate was adjusted so that the output on a quartz crystal monitor was constant from run to run. Because the instantaneous deposition rates of higher fluence runs were higher than those of the lower fluence runs, it was necessary to approximately double the pulse rate during the low fluence runs. We previously showed[14] that the influence of the instantaneous deposition rate F_{inst} at constant average deposition flux is small, having a dependence of $F_{inst}^{0.034}$. Doubling the instantaneous deposition flux at constant average deposition rate would therefore be expected to give a difference in percolation thickness of only about 2.5%. This is considerably less than the differences shown between the two panels in Fig. 1 above 135 °C, so we can be confident that the effect of varying the pulse duration had no impact on our results.

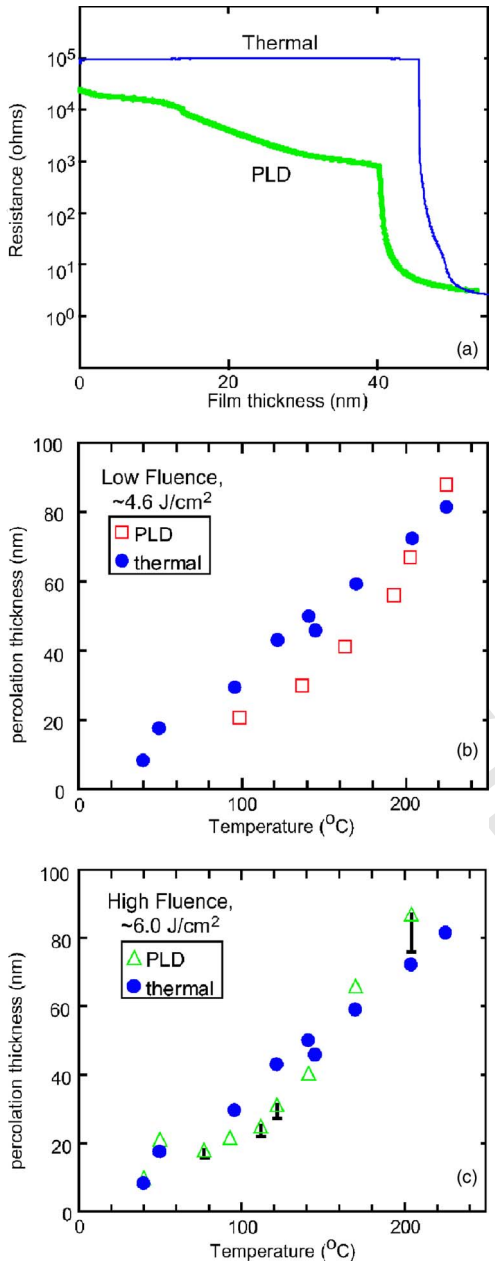

FIG. 1. (Color online) (a) Representative resistance measurements vs film thickness for high-fluence PLD (thick line) and thermal (thin line) runs. These runs were performed at 135 °C. The electrical percolation transition appears as a dramatic change in the slope of the curve, resulting in a resistance drop of at least an order of magnitude. Note that the measurement is not precise for high resistance; considerable scatter is observed in the initial, predeposition resistance, completely independent of deposition method. No systematic effect of this behavior was observed in the percolation thickness measurement. [(b) and (c)] Film thickness at electrical percolation vs temperature for PLD [squares in (b), triangles in (c)] and thermal deposition (filled circles). For PLD runs, laser fluence is approximately 4.6 J/cm^2 in (b) and 6 J/cm^2 in (c). Possible error in percolation thickness is <7% for all data points, as discussed in text; error bars are not shown. The average deposition flux was 0.06 nm/s. For the four runs in (c) performed at a lower average flux, error bars indicate correction due to scaling by $F^{-0.33}$, as discussed in text.

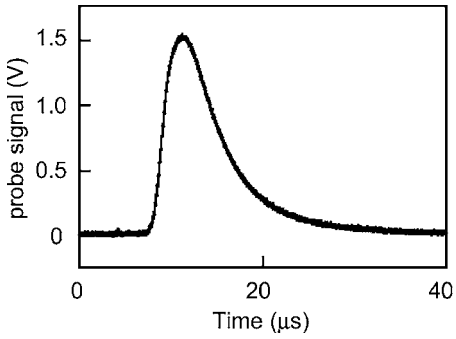

FIG. 2. Representative TOF ion probe signal, recorded in vacuum 10 cm from the target, at a probe bias of −15 V. The signal is averaged over 20 laser pulses. The laser pulse occurred at 4 μs. The kinetic energy calculated for the peak of the distribution is about 105 eV. The laser fluence was approximately 5 J/cm^2.

In Fig. 3, we show the morphological progression from equiaxed clusters to elongated coalescing clusters to a percolating film to the filling in of pinholes that characterized our grown films. The films in Fig. 3 are Ag films grown on mica at 200 °C,[15] grown at an average deposition rate of 0.25 nm/s by thermal deposition and by PLD at 20 Hz at approximately 5 J/cm^2. As can be seen, both undergo a similar progression, but the PLD films (left column) at comparable morphological stages are thicker and exhibit higher roughness.

Several interesting observations emerge from Fig. 1. First, comparing the PLD results of panels (b) and (c), we find that the effect of increasing the fluence from 4.6 to 6 J/cm^2 at constant F appears to shift the PLD curve to lower tempera-

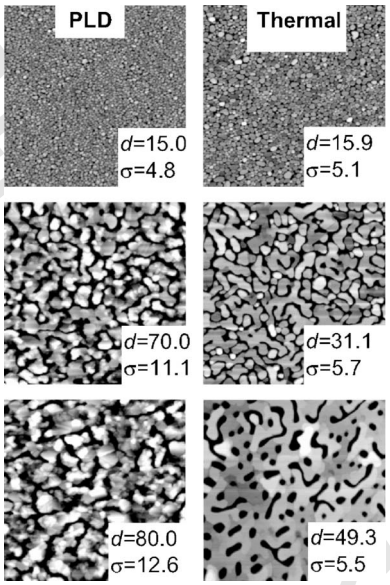

FIG. 3. Morphological progression for Ag/Mica films grown at 200 °C by PLD (left column) and thermal deposition (right column). All scans are 5×5 μm^2. Thickness (d) and rms roughness (σ) values in nm are provided for each image. The roughness values are calculated only for the Ag, with the substrate excluded using A manual threshold of the image. The roughness values have possible error of ±10%. Adapted from Ref. 12.

ture by about 30 °C. Additionally, at sufficiently low temperature, PLD films percolate sooner than thermally deposited films, but with increasing temperature a regime is entered in which PLD films percolate later than thermally deposited films, consistent with the observation of Fig. 3. This latter regime warrants further scrutiny, especially because it is at odds with the predictions of the KMC simulations that, considering only the time structure of the flux, PLD films should percolate sooner, or with relatively *less* deposition. One important result of Fig. 3 is that the islands of PLD films are indeed, as predicted by the simulations, smaller and more densely spaced than those of the thermally deposited films. This demonstrates that the discrepancies between experiment and simulation are not simply due to unanticipated trends in island size. We previously reported ion probe measurements of high kinetic energies—105 eV at the peak of the TOF ion distribution and 250 eV at the high end.[12] The implication is that the morphological evolution of Ag islands grown by PLD is governed not only by the kinetics associated with the flux pulsing but also by the energetic character of the depositing PLD species. Hence, we search for the origin of the delayed onset of percolation in PLD films in the energetic characteristics of the flux.

B. Systematic variation of kinetic energy

The influence of kinetic energy on percolation thickness was investigated with two separate methods for varying the kinetic energy of the depositing species: introducing an inert background gas into the chamber and varying the laser fluence. The first method used to modify the kinetic energy of the depositing species was to perform depositions in varying pressures of ultrahigh purity He. The gas was leaked into the chamber at a controllable rate maintained by a mass flow controller (DynaMass). The pressure was monitored with a Pirani gauge. Because the deposition rate varies with fluence due to changes in processes such as resputtering, a constant deposition rate was maintained by partially obstructing the beam with an aperture so as to maintain a constant average deposition rate but still hold fluence constant. The resulting percolation thickness is plotted against background gas pressure (top axis) in Fig. 4 (crosses). A nonmonotonic behavior of the percolation thickness with decreasing kinetic energy (increasing pressure) is observed: the percolation thickness first drops, then rises with increasing pressure, toward the percolation thickness of a thermally grown film. A similar behavior was observed for films grown at 122 °C, 0.03 nm/s.[14] We do not understand the behavior at high He pressure, but we note that this regime provides kinetic energies below 30 eV. In this study, we focus on the behavior at low pressure, with kinetic energy above 30 eV.

The mean free path λ for energetic Ag in a gas of much more slowly moving He at temperature T and pressure P, for gas molecules of radius r_{He} and r_{Ag} (r_{He}=0.049 nm, r_{Ag} =0.165 nm), may be estimated using

$$\lambda = \frac{RT}{\pi(r_{He} + r_{Ag})^2 N_A P}, \quad (1)$$

where R is the universal gas constant and N_A is Avogadro's number.[16] Using Eq. (1), for a target-to-substrate distance of 10.5 cm, the expected numbers of collisions with He atoms for a given Ag atom prior to deposition are 5.3 and 18.4 for the lowest and highest He pressures studied, 29 and 100 mTorr, respectively.[17] The measured retained kinetic energies at these pressures, 80% and 40%, respectively, suggest that most collisions are grazing.[14]

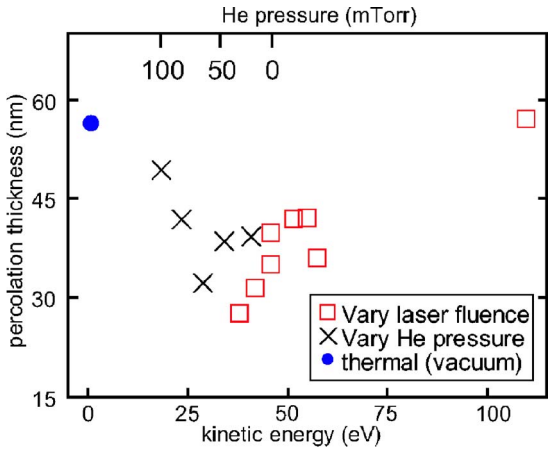

FIG. 4. (Color online) Ag on SiO_2 percolation thickness vs peak TOF kinetic energy for runs at 160 °C, with an average deposition rate of 0.06 nm/s, using two different schemes of varying the kinetic energy: by introducing background He gas (crosses) and by varying the laser fluence in vacuum (squares). The thermal point, interpolated from the data in Fig. 1, is shown for reference as a filled circle. The point at 110 eV is also interpolated from the data points in Fig. 1(c) at 141 °C (40.5 nm) and 170 °C (66.1 nm).

The second method used to modify the kinetic energy was to adjust the output voltage to the laser discharge. This varies the energy of the beam and, at constant spot size, permits control of the fluence supplied to the target. Supplying a higher energy density to the target is known to increase the kinetic energy of the species in the plume, as was confirmed in this case with a TOF ion probe measurement.[14] Again, the beam was obstructed with a progressively larger aperture in such a way that the higher fluence runs would have the same deposition rate. With the kinetic energy being varied in two ways, either by varying the background gas pressure or by varying the laser fluence, the percolation thickness varied with TOF-peak kinetic energy, as shown in Fig. 4. Table I provides the complete set of conditions used to generate each of the points in Fig. 4. Note that the data point at 110 eV is interpolated from the PLD data in Fig. 1(c).[18]

Starting from the pair of boxes at 46 eV in Fig. 4 and going down to the lowest box, at 38 eV, the data appear to diverge depending on whether kinetic energy is reduced by means of laser fluence reduction (boxes) or background gas introduction (crosses). We determined with a TOF ion probe that the distributions of ion kinetic energies are comparable for the two cases, but we cannot make any statement regarding the energy distribution of neutral species. It is possible that there is a difference in film growth behavior in the presence of He arising from effects such as oblique incidence of depositing scattered species, but we did not investigate these differences. Nevertheless, both series show that for peak kinetic energy greater than 28 eV, increasing the kinetic en-

TABLE I. Percolation thickness vs pressure data presented in Fig. 4. $T=160$ C, $F=0.06$ nm/s.

Pressure (mTorr)	Fluence (J/cm^2)	Kinetic energy (eV)	Percolation thickness (nm)
Vacuum	3.98	38	27.6
Vacuum	4.04	42	31.4
Vacuum	4.24	46	35.0
Vacuum	4.24	46	39.7
Vacuum	4.38	51.5	41.8
Vacuum	4.51	55	42.0
Vacuum	4.77	57.4	36.0
Vacuum	6.0	110	57.0
29	4.24	41	39.3
48	4.24	34.2	38.5
63	4.24	28.7	32.3
83	4.24	23.4	41.8
100	4.24	18.4	49.4

ergy of the depositing species increases the percolation thickness. This result has several implications. With respect to the data in Fig. 1, it shows that the results of a PLD experiment are extremely sensitive to the conditions under which the experiment was run. Most importantly, Fig. 4 presents unambiguous evidence of an increasing percolation thickness with increasing kinetic energy above about 30 eV—the energy range of the PLD data in Fig. 3 and Figs. 1(b) and 1(c)—and explains the shift in the PLD curve with kinetic energy shown in Fig. 1. The focus now shifts to understanding the nature of this energetic effect in terms of atomistic energetic mechanisms.

IV. MODELING

Because films deposited by PLD exhibit the same morphological progression as do thermally deposited films, we seek to understand the differences in percolation thickness within the framework of the kinetic freezing model: percolation is still interpreted as a competition between island growth, which tends to drive the system toward impingement and percolation, and coalescence, which tends to drive the system away from percolation. From this perspective, a promising avenue of inquiry is to consider the possibility that the effect of energetic deposition is to modify the time for coalescence in some way. If, for example, energetic deposition could accelerate coalescence, then the thickness range over which coalescence would remain efficient relative to impingement would be extended and percolation would be delayed. To explore this possibility, simulations of systems of one and two islands under the presence of energetic defect creation were performed.

It is known that metal atoms depositing at kinetic energies greater than 10 eV can have several effects, including resputtering, insertion at step edges, adatom and/or vacancy pair creation, small island breakup, and hyperthermal diffusion.[19–25] The yields for these mechanisms have been quantified in molecular-dynamics (MD) simulations performed for Cu (111),[21,26] and the results obtained are also valid for Ag (111).[27] It has also been shown that implantation of metal atoms into insulating substrates can occur during PLD deposition.[28,29] Of these mechanisms, adatom-vacancy pair creation is deemed most promising as a means of explaining an acceleration in coalescence both because it occurs with a high yield (e.g., 1.6 adatom-vacancy pairs per incident ion at 110 eV) and because an enhanced formation rate of mobile adatoms is expected to accelerate surface-diffusion mediated coalescence. To investigate the effect of adatom-vacancy accelerated coalescence for kinetic energies greater than 30 eV, detailed simulations were performed, and this is the focus of this section.

A. Simulation description

To attempt to gain insight into the role that energetic effects could play in possibly accelerating coalescence, a different KMC program was developed in which energetic defect creation is allowed.[21,30,31] Unlike the nonenergetic simulations discussed above, in which the entire system—including deposition, island growth, and island coalescence—was incorporated into the simulation, this simulation instead focused on the detailed kinetics of the coalescence process itself, from the perspective of just two islands. The idea that energetic mechanisms are affecting the coalescence process is anticipated in two essential ways. First, only adatom-vacancy pair creation is allowed; other energetic defects are neglected. Note that when we use the term "adatom-vacancy pair creation," we refer specifically to the process by which the simulation explicitly creates an adatom-vacancy pair in response to an atomic impact; our use of this term does not refer to the thermal processes by which adatoms can diffuse out of a terrace or step edge, leaving behind a vacancy. Second, no actual deposition occurs during the simulations; instead, impacts from arriving atoms simply create adatom-vacancy pairs. Only the approach of two islands to equilibrium is monitored, and so roughening effects that arise from growth are omitted so as to prevent them from obscuring the underlying kinetics of the coalescence process with and without defect creation. We recognize that in the presence of deposition, the relative number of adatoms per vacancy would be higher, and so the effects we will report at specific adatom-vacancy pair creation rates may not be observed experimentally at corresponding rates. Our purpose is to ascertain whether the experimental results can be interpreted with a model that only incorporates this specific energetic mechanism apart from the base line thermal processes. Simulations are performed on an fcc (111) surface, with a system size of 200×200. Simple bond-counting kinetics is used, with the activation barrier to any transition being given by $nE_{AA}+mE_{SA}$, where n (m) is the number of bonds the atom shares with Ag (substrate) atoms, which have energy $E_{AA}(E_{SA})$. We set $E_{AA}=0.1154$ eV.[32] Using bond-counting kinetics is reasonable for Ag(111) because the barriers for hopping on a bare terrace and along a step edge are 67 and <300 meV, respectively, which are small compared to the barrier for vacancy

diffusion, 540 meV. An atom is allowed to occupy any site so long as it has at least one neighbor in one of the three "downward" directions. The explicit step-edge barrier is not included in these simulations, and atoms are only allowed to make nearest-neighbor jumps.

When adatom-vacancy pair creation occurs, the system randomly chooses a surface atom for the initial impact. For simplicity, an adatom-vacancy yield of one pair per atomic impact is assumed. For each impact, the adatom and surface vacancy are created independently. For each, a candidate defect creation site is chosen randomly within a circle surrounding the impact site and having a radius of $3a$, where a is the minimum lattice translation distance.[27] In practice, this gives 37 in-plane positions for possible defect creation, some of which may be vacant. If the chosen site cannot validly accommodate a defect of the desired type, the routine randomly selects from among the three equivalent neighboring out-of-plane nearest-neighbor displacements (up or down, depending on whether the potential creation site is occupied or unoccupied, respectively), and moves along this direction until it finds a new candidate site where the defect can be created. The candidate site for a vacancy must be within one lattice unit up or down from the impact site; the candidate site for an adatom must be within one unit up or down of the layer above the impact site. These rules simulate the effect that adatom-vacancy creation on average results in a net uphill flux arising from adatoms "popping out" of terraces. If this condition is met, the defect is created, and the surrounding atoms are alerted of the change. Otherwise, a different candidate site within the circle is chosen. If, after 60 tries, a suitable defect site cannot be found, a new site for the atomic impact is chosen and the process is repeated.

The system of a pair of coalescing islands is initialized as two spherical caps, in contact, with the long axis of the two-island system lying along the x axis. At each data taking step, the x, y, and z moments of the system are recorded according to

$$M_\alpha = \sqrt{\frac{\sum_{n=1}^{N} (r_{n,\alpha} - R_\alpha)^2}{N}}, \tag{2}$$

where α denotes the index (x, y, or z) of the moment being calculated and the sum runs over all of the Ag atoms in the simulation N, comparing the α coordinate of each with that of the true center of mass of the system $\vec{R}$, which is calculated at each data taking step. To monitor the system's progress toward coalescence, the ratio of the in-plane moments, which shall be referred to as the aspect ratio, is obtained by calculating

$$A = \frac{M_x}{M_y}. \tag{3}$$

The plot of A vs time is fitted with an exponential decay function to obtain the time constant associated with coalescence. Jensen and Combe previously reported that, for low temperature, the exponent of coalescence time with island size is not the classical value of 4, but can be much higher due to the presence of facets, which impede coalescence.[33] For $T=600$ K, the temperature used in our simulations, we observed that the time constant for coalescence went as $\tau \propto R^{4.53}$, which is reasonably consistent with the classical exponent of 4.0.

It is, at the outset, unclear whether the kinetic path followed by the islands toward equilibration will be affected by the presence of energetic mechanisms. It is therefore necessary to ensure that the islands do not, during coalescence, undergo a shape change (other than, obviously, the coalescence transition). This is achieved by maintaining the contact angle θ_{eq}, which entails controlling the ratio E_{SA}/E_{AA}. In these simulations, E_{SA}/E_{AA} was set to 0.975, which gave an equilibrium contact angle of 34°. As a test, single islands were simulated evolving out of nonequilibrium shapes. The islands reached θ_{eq} quickly compared to the time required for two-island systems to coalesce.[14]

B. Results

Two-island equilibration simulations were performed for an initial contact angle $\theta_0=30°$. In some simulations, the individual islands were "small," having an in-plane radius $R=19a$; in others, the islands were "large," with $R=25a$. In both cases, overlapping two-island systems were initialized by creating spherical caps that had a 1% overlap, which was accomplished by placing the center of mass of each spherical cap a distance of 99% of the basal radius from the center of mass of the two-island system. An individual island with $R=19a$ contains 4591 atoms; the corresponding two-island system contains 9161 atoms. For $R=25a$, an individual island contains 10 182 atoms, and the corresponding two-island system contains 20 341 atoms. The aspect ratio of the two-island system as a function of time was monitored.

The plot in Fig. 5 presents the aspect ratio of a pair of coalescing large islands ($R=25a$) as a function of time for several conditions: thermal, in which no defects are created, and thermal plus adatom-vacancy pair creation resulting from atomic impacts at rates $k_{a\text{-}v}$ of 1×10^5, 2×10^5, 5×10^5, and 1×10^6 pairs/s per site projected on the basal plane. Adatom-vacancy pair creation at 1×10^5 pairs/s behaves essentially the same as in the thermal case. It makes sense that below some threshold, the defect production rate is so low relative to thermally activated defect creation that the small quantity of additional surface diffusers yields no tangible impact on the coalescence process.[34]

To identify the threshold adatom-vacancy pair creation rate below which no difference from thermal evolution would be expected, the thermal adatom generation rate of a single island was calculated by considering an equilibrated thermal island evolving with no energetic defect creation active. To create terrace adatoms under thermal evolution, an adatom must be emitted from a step by hopping out of a kink site. To obtain κ, the total rate of thermal adatom generation for the system, the in-plane coordination i of every atom in the island was obtained from the simulation, and the hopping rate for each coordination k_i was multiplied by the number of atoms on the island having that coordination N_i, as

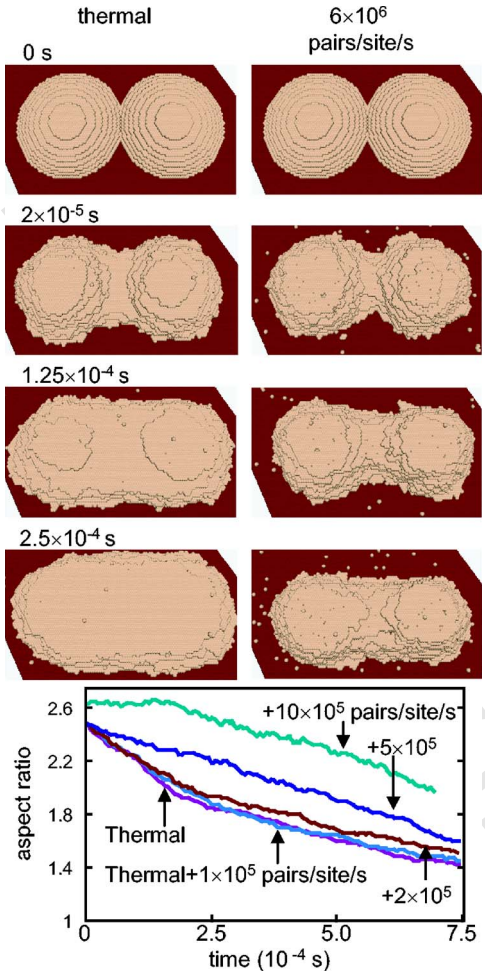

FIG. 5. (Color online) (Top) Evolution of two-island system with time with no defect creation (left column) and with adatom-vacancy pair creation at 1×10^6 pairs/site/s (right column). The initial individual island radius is $25a$. (Bottom) Change in aspect ratio [given by Eq. (3)] with time from KMC simulations at 600 K of two islands equilibrating, with several different adatom-vacancy pair creation rates: 0, 1×10^5, 2×10^5, 5×10^5, and 1×10^6 pairs/site/s. The results are averaged over three simulations.

$$\kappa = \sum_{i=1}^{6} N_i k_i, \tag{4}$$

where the sum runs from 1 to 6 because atoms with no in-plane neighbors are already on the terrace. Additionally, the sum only considers atoms in the second layer or higher, because atoms emitted from the first layer will, in general, become adatoms on the substrate, which do not factor into this analysis. Not all hops necessarily result in the creation of adatoms, so κ is an upper limit on the actual total thermal adatom creation rate. The total rate calculated from Eq. (4) for a typical thermal island was 7.6×10^8 adatoms/s. By comparison, multiplying the energetic adatom-vacancy pair creation rate of 1×10^5 pairs/site/s by the total number of possible impact sites on the island in question, which was about 1500 sites, gives the total energetic adatom-vacancy pair creation rate for the entire island, which was equal to 1.5×10^8/s, about 20% of κ.

The plot in Fig. 5 illustrates the striking result that coalescence appears to be *inhibited* rather than accelerated with increasing adatom-vacancy creation rate. This runs contrary to our initial hypothesis that suggested that, given that adatoms mediate coalescence, creating more adatoms should enhance the rate of coalescence.

The detailed morphology of the simulations is presented in Fig. 5 (top), which compares the progress toward coalescence of a two-island system under no defect creation (left column) and adatom-vacancy pair creation at 1×10^6 pairs/site/s (right column). The immediate conclusion from this figure is that adatom-vacancy pair creation retards the coalescence process. This implies that for a system of many islands, percolation would be expected to occur *sooner* in the presence of adatom-vacancy pair creation. Thus, the simulations do *not* support the argument that, for the cases where PLD films percolate later than thermal films, they do so due to the acceleration of coalescence because of the additional adatoms present to participate in coalescence.

The resolution of this puzzle lies in another aspect of Fig. 5. Initially, the two-island system is eight layers high. As the thermal system coalesces, it also relaxes vertically to reach a final height of four layers. In contrast, the system with adatom-vacancy pair creation remains eight layers high for the entire duration of the simulation. Below, we show that this is not simply a case of delayed coalescence resulting in a slower rate of vertical decay toward the same ultimate height; rather, the net uphill flux from adatom-vacancy pair creation is stabilizing the vertical shape of the islands.

We performed simulations of the evolution of a single spherical cap island. In Fig. 6, we show the z-moment evolution with time for conditions of no adatom-vacancy creation and adatom-vacancy creation at various rates. The thermal island, which starts the simulation as a spherical cap with contact angle of 30° and $R=19a$, approaches the equilibrium contact angle of 34° very quickly, and the z-moment of the island relaxes over a somewhat extended period to an equilibrium value. Adatom-vacancy pair creation at 1×10^6 pairs/site/s appears to represent a critical value; below this rate, the islands relax to the equilibrium shape, though the rate of relaxation decreases as the defect creation rate increases. At 1×10^6 pairs/site/s, though, the initial vertical moment of the island persists over the duration of time studied. At higher rates, the vertical moment *increases* with time. The island snapshots of Fig. 6 (top) show the shape evolution of a single island in more detail. The left column shows thermal evolution, and as mentioned above, the island relaxes with time to a flatter, wider shape. In contrast, the island of the middle column, in which adatom-vacancy pairs are created at a rate of 1×10^6 pairs/site/s, does not change its height or its shape, apart from fluctuating around its initial shape. Finally, the island in the right column, subjected to adatom-vacancy pairs at a rate of 6×10^6 pairs/site/s, grows vertically with time, and also contracts laterally.

Vertical growth in a stepped island such as this requires the formation of new layers on top of the existing layers. This can occur, in principle, by thermal creation of adatoms followed by island nucleation, but in practice this process is

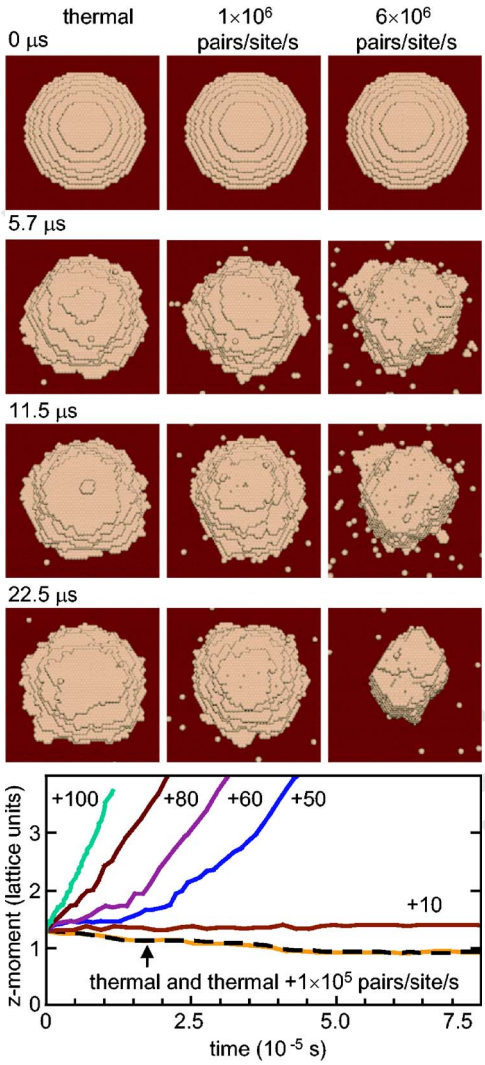

FIG. 6. (Color online) (Top) Evolution of a single island, $R_0=19a$, in the presence of no defects (left column), 1×10^6 pairs/site/s (middle column), and 6×10^6 pairs/site/s (right column). (Bottom) z-moment evolution with time for adatom-vacancy creation at various rates: 0, 1×10^5, 1×10^6, 5×10^6, 6×10^6, 8×10^6, and 1×10^7 pairs/site/s. The 1×10^5 pairs/site/s and thermal runs are essentially identical and show slight vertical relaxation (from six layers initially to four layers). The 1×10^6 pairs/site/s run exhibits neither relaxation nor growth; higher than this rate, the islands grow vertically, and the time over which growth occurs decreases as the creation rate increases.

exceedingly slow. In contrast, atomic impacts kick adatoms "up" out of terraces athermally and rapidly. Vertical contraction, on the other hand, requires the removal of unfavorably high layers. As the left-hand side of Fig. 6 shows, there is no bottleneck to downhill transport. The adatom-vacancy pair creation mechanism may modestly increase the rate of downhill transport, but appears to vastly increase the rate of uphill transport. We expect high enough point defect creation rates to provide a sufficiently high concentration of adatoms on the topmost terrace that stable two-dimensional layers are formed.[14]

This analysis suggests that at high enough rates, the net uphill flux from adatom-vacancy pair creation can induce a

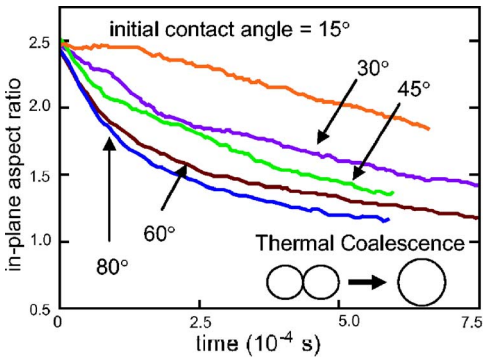

FIG. 7. (Color online) Aspect ratio vs time for two-island systems evolving with no defect creation. Islands initially have contact angles of, from top to bottom, 15°, 30°, 45°, 60°, and 80°. The equilibrium contact angle is 34° for all runs. The plots are averages of three simulations.

shape change that causes the individual islands to become taller. To consider what impact this should have on coalescence, we returned to two-island coalescence simulations. In these simulations, the initial contact angle of the constituent islands was varied, but the total volume of the system and the equilibrium contact angle (34°, controlled by the ratio E_{SA}/E_{AA}) were held constant for all runs. A two-island system, having a total volume of 20 341 atoms, was allowed to evolve with *no adatom-vacancy pair creation* operating. As Fig. 7 shows, coalescence proceeds faster for the initially taller islands. This result is reasonable considering that coalescence in these simulations occurs by a process whereby, for a given layer, the two separate "terraces" in that layer evolve to touch one another by step fluctuations. Given that the corresponding steps are closer together for taller islands of the same volume, this process can occur more quickly in the tall islands.

The simulations that led to Fig. 7 were performed with no adatom-vacancy pair creation to reflect the experimental fact that defects are created during the 10^{-5} s or so that the pulse is on, but that coalescence is occurring on a time scale comparable to the time between pulses, on the order of 10^{-1} s. (Based on the results of Ref. 12, this must be the case, or else there would be no difference between runs performed at different frequencies with $f<40$ Hz.) If most of the coalescence occurs without defect creation operative, then simulating coalescence with no defect creation can still be considered applicable to PLD. The crucial point is that the effect of adatom-vacancy pair creation is, based on Fig. 6, to induce a shape change in the islands that makes them more vertical than the corresponding islands evolving without defects. These islands can then coalesce more quickly by virtue of being taller, as shown as Fig. 7. This would accelerate coalescence, thus delaying percolation, and this two-step mechanism therefore provides a plausible explanation for why films grown in the presence of enhanced adatom-vacancy pair creation would require more deposition to reach percolation.

This scenario is plausible as an explanation for the delayed onset of percolation evident in the high-temperature range of Fig. 1, and as kinetic energy is increased in Fig. 4.

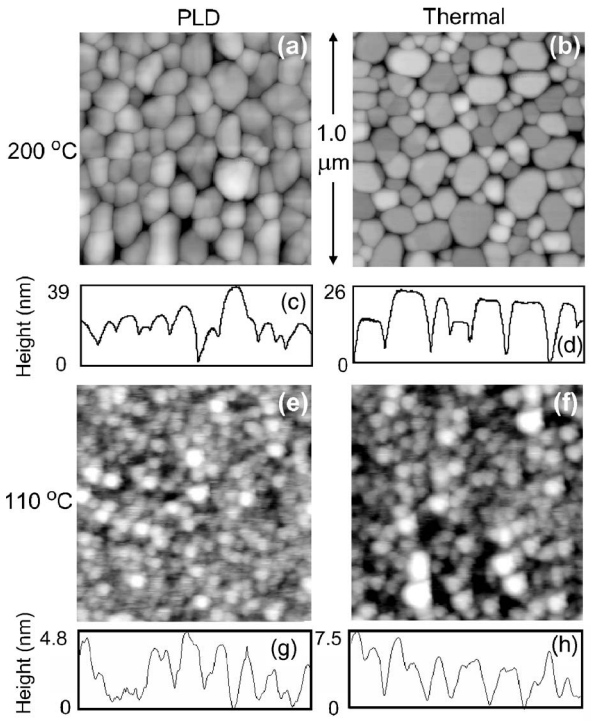

FIG. 8. AFM images of PLD islands (left column) and thermal islands (right column). (a) and (b) are Ag/Mica films grown at 200 °C, and both are 15 nm thick. (e) and (f) are Ag/SiO_2 films grown at 110 °C, and both are 6 nm thick. (c) and (d) are single line traces for (a) and (b), and (g) and (h) are single line traces for (e) and (f), respectively. The difference in island shape is more dramatic between (a) and (b) than between (c) and (d).

Because coalescence occurs so rapidly on the time scale of experiments, a detailed real-time study of coalescence in the presence of defect creation mechanisms is beyond the scope of this research but is accessible, in principle, with various time-resolved diffraction studies. However, this argument is supported by *ex situ* AFM images of the film morphologies after quenching to room temperature. Figure 8 shows a comparison of AFM images for PLD and thermal films grown under nominally identical conditions. In Figs. 8(a) and 8(b) are Ag/mica at 200 °C, a case where PLD films percolate later than thermally deposited films. In Figs. 8(e) and 8(f) are Ag/SiO_2 at 110 °C, a case where PLD films percolate sooner than thermally deposited films. At both temperatures, PLD films have a higher total island density. Also shown are representative line traces from these images. The shape difference between the islands at 200 °C is more pronounced than the difference between the island shapes at 110 °C. The thermal islands in (b) have flat tops, in contrast to the much more rounded PLD islands of (a), possibly indicating that the islands of the thermally grown film had insufficient vertical transport to achieve a fully rounded shape on top. In contrast, there is no discernable shape difference at 110 °C. This observation supports the notion that when PLD percolates later than thermal deposition, the explanation lies in a shape transition (to more vertical islands) from the uphill flux induced by the kinetic energy. Under all conditions, the initial PLD island density remains higher than in thermal deposition, but under certain conditions, it appears that the acceleration in coalescence due to a shape change in the islands is more important than the initial island density in determining the overall percolation behavior.

We do not fully understand why the delay in percolation associated with kinetic energy should be observed at the upper rather than the lower range of our substrate temperatures. We conjecture that a possible explanation lies in the larger island size at high temperature. The energetically induced uphill flux is related to the deposition flux and does not depend strongly on the island size, but the rate of relaxation is much lower for larger islands. Although the rate of thermally activated coalescence will also be higher at high substrate temperature, the island size may be sufficiently large at high temperature that the islands retain the pair-creation-induced height increase over a longer period of time than do the smaller islands observed at low substrate temperature. The longer the increased height of a given island is retained, the more of an impact this can have on the coalescence process. Preliminary simulation results suggest conditions under which this delayed relaxation of larger islands at higher temperature is observed. We expect that as temperature is increased further—beyond the range that was accessible in these experiments—eventually, thermally activated transport would overwhelm the energetic effect and the PLD percolation thickness would again approach the thermal percolation thickness, but we did not pursue this limit.

Under the scenario described above, the effect of the kinetic energy induced uphill flux on percolation is most evident at intermediate temperature: at low temperature, it is reduced in importance by the small island size and is overwhelmed by the flux pulsing effect on nucleation; at intermediate temperature, it is enhanced in importance by the large island size; and at sufficiently high temperature, it would be overwhelmed by thermal point defect processes.

V. SUMMARY

This paper presents a controlled experimental and multifaceted KMC study into the difference between PLD and thermal metal-on-insulator deposition. The initial hypothesis, motivated by KMC simulations, was that the most significant difference between these two techniques was associated with the flux pulsing of PLD. The high instantaneous deposition rate was expected to lead to a very high island density, which, in turn, would result in faster advancement through the characteristic metal-on-insulator morphological progression. Previously reported KMC simulations that treated only this nonenergetic aspect of the flux, and which permitted binary island-island coalescence, motivated this prediction.

Experiments were performed over a range of temperatures using thermal deposition, a PLD deposition series at low fluence, and a PLD deposition series at high fluence. At sufficiently low temperature, PLD films percolated sooner than did thermally deposited films, as predicted. Under certain conditions, however, PLD films percolated later. These conditions are reflected in a crossing in the PLD and thermal percolation vs temperature curves of Fig. 1—a crossing that occurs at different temperatures for the two fluences investigated.

The cases where PLD films percolate later than thermal films cannot be explained by flux pulsing alone, and the energetic character of the pulse must be taken into account. We observed experimentally that as the kinetic energy of the depositing species was increased by two different methods in the range between 28 and 110 eV, the percolation thickness increased. The most likely mechanism appears to be a delay in percolation due to enhanced coalescence arising from adatom-vacancy pair creation, which occurs with increasing yield for increasing kinetic energy.

Detailed KMC simulations were performed to investigate two-island coalescence in the presence of varying rates of adatom-vacancy pair creation. Surprisingly, adatom-vacancy pair creation was observed to *retard* the rate of coalescence by inducing a net uphill flux that causes a shape change in which the islands become more vertical. A series of two-island coalescence simulations with no adatom-vacancy pair creation was then performed, with the independent variable being the initial contact angle of the constituent islands and the equilibrium contact angle with the substrate held constant for all simulations. Taller-than-equilibrium islands were observed to coalesce more rapidly than the islands that were closer to the equilibrium shape. These observations suggest a mechanism by which the delayed percolation of PLD films can be explained: (1) the energetic deposition results in a net uphill flux that induces a vertical shape change; (2) the more vertical islands coalesce more rapidly; (3) the result is an extended time period over which coalescence is efficient compared to island-island impingement for energetic deposition; and (4) the percolation transition is delayed. AFM images of experimental films confirmed that the PLD islands are more vertical than the thermal islands when PLD films percolate later than thermal films.

We conclude that for low temperature, the high island density of PLD dominates the morphology evolution, and PLD films reach percolation sooner than thermal films. As the temperature is increased, the PLD percolation thickness approaches and then exceeds the thermal percolation thickness, indicating the increasing importance of an energetic effect. This effect could plausibly result from accelerated coalescence associated with an energetically induced vertical shape transition in the islands. An important direction for future research is the development of a quantitative and predictive model for this trade-off.

ACKNOWLEDGMENTS

This research was supported by NSF Grant No. DMR-0306997. We gratefully acknowledge helpful discussions with Zhenyu Zhang, Josh Pomeroy, Efthimios Kaxiras, Julian Carrey, Craig Arnold, Gwo-Ching Wang, and Jonah Erlebacher and technical assistance from Stephen Shepard and John Chervinsky.

*Present address: Benét Laboratories, 1 Buffington Street B115, Watervliet, NY 12180. FAX: (617) 496-9837. Email address: jwarrend@post.harvard.edu

[1] D. W. Pashley, M. H. Jacobs, M. J. Stowell, and T. J. Law, Philos. Mag. **10**, 127 (1964).
[2] A. A. Baski and H. Fuchs, Surf. Sci. **313**, 275 (1994).
[3] G. Jeffers, M. A. Dubson, and P. M. Duxbury, J. Appl. Phys. **75**, 5016 (1994).
[4] X. Yu, P. M. Duxbury, G. Jeffers, and M. A. Dubson, Phys. Rev. B **44**, 13163 (1991).
[5] P. Brault, A.-L. Thomann, and C. Andreazza-Vignolle, Surf. Sci. **406**, L597 (1998).
[6] J. S. Biteen, D. Pacifici, N. S. Lewis, and H. A. Atwater, Nano Lett. **5**, 1768 (2005).
[7] J. S. Biteen, N. S. Lewis, H. A. Atwater, H. Mertens, and A. Polman, Appl. Phys. Lett. **88**, 131109 (2006).
[8] Grain boundaries do not affect this picture very significantly when the boundary energy is much less than the metal free surface energy. The dihedral angles of grain boundary grooves in Ag vary from 160° to 175°, according to A. P. Greenough and R. King, J. Inst. Met. **79**, 415 (1951).
[9] F. A. Nichols and W. W. Mullins, J. Appl. Phys. **36**, 1826 (1965).
[10] D. B. Chrisey and G. K. Hubler, *Pulsed Laser Deposition of Thin Films* (Wiley, New York, 1994).
[11] P. R. Willmott, Prog. Surf. Sci. **76**, 163 (2004).
[12] J. M. Warrender and M. J. Aziz, Appl. Phys. A: Mater. Sci. Process. **79**, 713 (2004).
[13] S. K. So, H. H. Fong, C. F. Yeung, and N. H. Cheung, Appl. Phys. Lett. **77**, 1099 (2000).
[14] J. M. Warrender, Ph. D. thesis, Harvard University, 2004.
[15] A different calibration of the thermocouple measurement was used during this experiment than those throughout the rest of the paper. The actual temperature was probably closer to 180 °C.
[16] F. Reif, *Fundamentals of Statistical and Thermal Physics* (McGraw-Hill, Boston, 1965).
[17] This equation is appropriate for the limit in which the Ag atoms have much higher average speed than He atoms. Ag ions with 55 eV of kinetic energy have an average speed of 9560 m/s and He atoms at 300 K have an average speed of 1380 m/s, so the actual average number of collisions for a Ag atom may be slightly higher than indicated by Eq. (1).
[18] If the percolation thickness at 110 eV, 160 °C, were significantly lower than the interpolated value, this would introduce several elbows to the PLD curve in Fig. 1(c) (triangles). This would be a highly unexpected result.
[19] T. N. Hansen, J. Schou, and J. G. Lunney, Europhys. Lett. **40**, 441 (1997).
[20] S. Fahler, K. Sturm, and H.-U. Krebs, Appl. Phys. Lett. **75**, 3766 (1999).
[21] J. M. Pomeroy, J. Jacobsen, C. C. Hill, B. H. Cooper, and J. P. Sethna, Phys. Rev. B **66**, 235412 (2002).
[22] J. Jacobsen, B. H. Cooper, and J. P. Sethna, Phys. Rev. B **58**, 15847 (1998).
[23] C. M. Gilmore and J. A. Sprague, Phys. Rev. B **44**, 8950 (1991).
[24] P. R. Willmott, R. Herger, C. M. Schlepütz, D. Martoccia, and B. D. Patterson, Phys. Rev. Lett. **96**, 176102 (2006).

[25] T. Diaz de la Rubia, R. S. Averback, R. Benedek, and W. E. King, Phys. Rev. Lett. **59**, 1930 (1987).
[26] J. Pomeroy, Ph. D. thesis, Cornell University, 2002.
[27] J. Pomeroy (private communication).
[28] J.-P. Barnes, A. K. Petford-Long, A. Suarez-Garcia, and R. Serna, J. Appl. Phys. **93**, 6396 (2003).
[29] S. Fahler, S. Kahl, M. Weisheit, K. Sturm, and H. U. Krebs, Appl. Surf. Sci. **154-155**, 419 (2000).
[30] M. Strobel, K.-H. Heinig, and T. Michely, Nucl. Instrum. Methods Phys. Res. B **178**, 105 (2001).
[31] M. E. Taylor and H. A. Atwater, Appl. Surf. Sci. **127-129**, 159 (1998).
[32] This value was chosen because it gave the best fit to the full set of barriers calculated in Ref. 26 using the embedded atom method. While those barriers were calculated for Cu(111), we chose them as the target for our fit because they were all obtained during the same calculation, and this internal consistency seemed more important given our goal of understanding experimental trends as opposed to making detailed predictions about Ag specifically.
[33] P. Jensen and N. Combe, Comput. Mater. Sci. **24**, 78 (2002).
[34] Only adatom motion is considered to mediate coalescence due to the very high barrier to vacancy motion under bond-breaking kinetics at this temperature.